AIAA JOURNAL
Vol. 41, No. 3, March 2003

Technical Notes

TECHNICAL NOTES are short manuscripts describing new developments or important results of a preliminary nature. These Notes cannot exceed six manuscript pages and three figures; a page of text may be substituted for a figure and vice versa. After informal review by the editors, they may be published within a few months of the date of receipt. Style requirements are the same as for regular contributions (see inside back cover).

Acoustic and Entropy Pulses Created in Duct Flows by Rapid Local Events

Miklos Sajben*
University of Cincinnati, Cincinnati, Ohio 45221
and
Gary L. Cole† and John W. Slater‡
NASA John H. Glenn Research Center at Lewis Field, Cleveland, Ohio 44135

Nomenclature

a	=	speed of sound [$=\sqrt{(\gamma p/\rho)}$ for a perfect gas]
B	=	strength of area disturbance [Eq. (38)]
c_v	=	specific heat at constant volume
D	=	characteristic transverse dimension of duct
H	=	total energy
I	=	strength of acoustic pulse [Eq. (13)]
J	=	strength of entropy pulse [Eq. (20)]
M	=	Mach number
P	=	total momentum
p	=	static pressure
Q	=	heat added to gas
q	=	heat flow into gas per unit duct length
R	=	perfect gas constant
S	=	cross-sectional area of duct
s	=	entropy per unit mass
T	=	absolute temperature
t	=	time
u	=	velocity
W	=	total mass
x	=	streamwise coordinate
γ	=	ratio of specific heats
Δ	=	change imposed during trigger event
λ	=	length of pulse or trigger device
ρ	=	density of gas
τ	=	duration of pulse or trigger event

Subscripts

B	=	associated with bump
E	=	associated with entropy pulse
i, f	=	initial and final values, resp.
mx	=	maximum value
t	=	related to trigger process
1, 2	=	upstream and downstream ends of control volume, respectively
$-$	=	associated with upstream-moving (left) acoustic pulse
$+$	=	associated with downstream-moving (right) acoustic pulse

Superscripts

$\bar{(\ )}$, $(\ )'$	=	undisturbed and disturbance quantity, respectively
$\dot{(\ )}$	=	time rate of change

Received 11 August 2001; revision received 16 October 2002; accepted for publication 18 November 2002.

*Professor Emeritus, Department of Aerospace Engineering and Engineering Mechanics; mmsajben@fuse.net. Fellow AIAA.
†Retired; glcdyc@apk.net.
‡P.E. Inlet Branch, MS 86-7; John.W.slater@grc.nasa.gov. Senior Member AIAA.

Introduction

SHORT-DURATION disturbances (pulses) can occur in constant-area duct flows for a variety of reasons: explosions, electric sparks, ignition processes, abrupt addition of heat caused by a malfunctioning electric circuit or unwanted chemical reaction, also an accidental deformation or rupture of a duct wall. Pulses can also occur as by products of an intended process, for example, strong pressure pulses accompany the pumping of pulsed lasers. Pulses can also serve as elements of diagnostic processes. One example is the impulse method used in acoustics to determine the impedance of various duct elements by creating a pulse and measuring its reflection from the element.[1] This method was used recently in two separate experiments to measure the acoustic impedance of operating compressors,[2,3] with the ultimate goal of formulating exit boundary conditions for high-speed inlet flow computations. The calculation method presented in this Note was of critical importance in developing the devices needed to create the required large-amplitude pulses.[4,5]

An approximate method is offered for the prediction of the properties of pulses created by a wide variety of stimuli. The theory is one-dimensional and linearized and characterizes pulses in integral terms. The resulting formulas allow calculations with a back-of-the-envelope simplicity. The method is useful as an engineering tool, and it also yields surprising insights into the distribution of energy among the pulses generated.

Problem Definition

It is well known that disturbances of compressible flows can be split into acoustic, entropy, and vorticity components. If the mean flow is nearly parallel, uniform, and if the disturbances are small, then the various disturbance types are independent of each other.[6] This Note focuses on disturbances in a constant-area duct containing a steady subsonic flow of an inviscid and thermally nonconducting perfect gas. The description is one-dimensional, which prevents considerations of vorticity but includes acoustic and entropy disturbances.

It is assumed that an abrupt "trigger event" occurs over an interior duct segment having a finite length λ_t that is comparable to D, during a finite time interval τ_t that is comparable to $D/\bar{a}$. Such an event can be induced in many different ways, but in each case some combination of excess mass, momentum, and energy is introduced into the system. The trigger event will initiate two acoustic pulses (waves), one propagating upstream (left) and one propagating downstream (right) at speeds $(\bar{u}-\bar{a})$ and $(\bar{u}+\bar{a})$, respectively. In general, an entropy pulse (wave) is also created that is convected downstream at speed u. All pulses have lengths comparable to D. Interest is confined to a control volume (CV) enclosing a finite duct length and to a finite time interval within which the entire transient occurs (Fig. 1). The flow properties are constant everywhere except within the pulses.

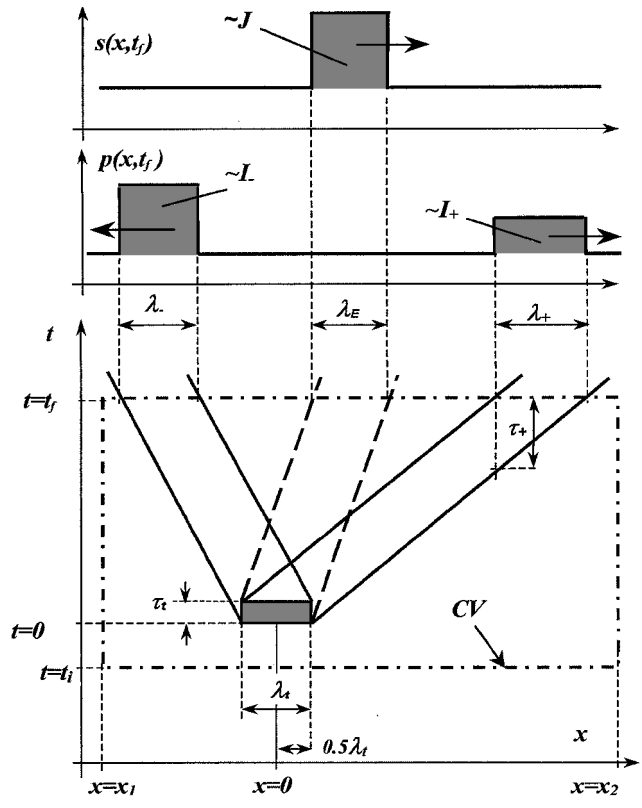

Fig. 1 Distance–time diagram of pulses created by a trigger event occurring in the space–time region shown shaded in the bottom part of the figure. Pulses are shown as square waves for simplicity. Shaded regions at top are proportional to the respective pulse strengths.

Characterization of Pulses

The mass conservation law requires that the mass added to the CV in the trigger event be equal to the sum of mass disturbances associated with the resulting three pulses. Analogous requirements apply to momentum and energy. These statements can be formalized if expressions are available for the mass, momentum, and energy associated with individual acoustic and entropy pulses. These are developed next.

The conservation of mass is expressed by the one-dimensional continuity equation

$$\frac{\partial \rho}{\partial t} + \frac{\partial}{\partial x}(\rho u) = \dot{\rho} \tag{1}$$

where $\dot{\rho}$ represents the local rate of addition of mass. Multiplying by $S\,\mathrm{d}x$ and integrating over the length of the CV, we get

$$\frac{\mathrm{d}}{\mathrm{d}t}\int_{\mathrm{CV}} \rho S\,\mathrm{d}x + [\rho u S]_1^2 = \int_{\mathrm{CV}} \dot{\rho} S\,\mathrm{d}x = \dot{W} \tag{2}$$

Because the choice of the CV is such that the ends of the x region are undisturbed, the flux terms in square bracket are those associated with the steady flow and hence cancel. The integral expression at left is the total mass within the CV, allowing Eq. (2) to be rewritten as

$$\frac{\mathrm{d}W}{\mathrm{d}t} = \dot{W} \tag{3}$$

Integrating over the finite time interval from t_i to t_f, we have

$$W_f - W_i = \int \dot{W}\,\mathrm{d}t = \Delta W \tag{4}$$

All quantities are linearized by splitting them into sums of steady and unsteady components, assuming the latter to be small. The linearized version of the preceding relation is

$$W_f' - W_i' = \Delta W, \qquad \text{where} \qquad W' = \int_1^2 \rho' S\,\mathrm{d}x \tag{5}$$

Analogous considerations lead to similar relations for momentum and total internal energy:

$$P_f' - P_i' = \Delta P, \qquad \text{where} \qquad P' = \int_1^2 (\bar{\rho}u' + \rho'\bar{u}) S\,\mathrm{d}x \tag{6}$$

$$H_f' - H_i' = \Delta H, \quad \text{where} \quad H' = \int_1^2 \left(\frac{p'}{\gamma - 1} + \bar{\rho}\bar{u}u' + \frac{1}{2}\rho'\bar{u}^2\right) S\,\mathrm{d}x \tag{7}$$

The integrands in Eqs. (5–7) differ from zero only in regions occupied by a pulse. Each integral over the entire CV consists of three discrete contributions; one from each pulse, each being an integral taken over the length of the pulse. In the absence of external disturbances, these integrals remain constant during the motion of each pulse and clearly represent integral properties of the respective pulses.

Acoustic Pulses

The flow property variations in the interiors of the pulses are isentropic, and the following relations hold:

$$\rho' = (1/\gamma)(p'/\bar{p})\bar{\rho} = p'/\bar{a}^2 \tag{8}$$

The momentum equation can be used to show that the velocity and pressure changes across an acoustic wave are related by the equation

$$u' = \pm p'/\bar{\rho}\bar{a} \tag{9}$$

where the plus and minus signs apply to right- or left-moving disturbances, respectively. Using Eqs. (8) and (9) to eliminate u' and ρ' from the integrals of Eqs. (5–7), the desired expressions for the mass, momentum, and energy associated with acoustic pulses are obtained:

$$W_\pm' = \frac{1}{\bar{a}^2} I_\pm \tag{10}$$

$$P_\pm' = \frac{(\bar{M} \pm 1)}{\bar{a}} I_\pm \tag{11}$$

$$H_\pm' = \left[\left(1 + \frac{\gamma - 1}{2}\bar{M}^2\right) \Big/ (\gamma - 1) \pm \bar{M}\right] I_\pm \tag{12}$$

where

$$I = \int p' S\,\mathrm{d}x \tag{13}$$

The mass, momentum, and energy of an acoustic pulse are all proportional to the quantity I, which is the volume integral of the pressure disturbance and will be referred to as the "strength" of the acoustic pulse. It has the dimension of energy, and it is proportional to the area under the pressure disturbance vs distance plot for the pulse, as illustrated in Fig. 1.

Entropy Pulses

The flow property variations in the interiors of entropy pulses obey the relations

$$p' = u' = 0 \tag{14}$$

$$\rho' = -(\bar{\rho}/\bar{T})T' \tag{15}$$

$$s' = R\{[\gamma/(\gamma - 1)](T'/\bar{T}) - p'/\bar{p}\} \tag{16}$$

Using these expressions to eliminate u' and ρ' from Eqs. (5–7), we get

$$W_E' = -[(\gamma - 1)/\bar{a}^2]J \tag{17}$$

$$P_E' = -[(\gamma - 1)\bar{M}/\bar{a}]J \tag{18}$$

$$H_E' = -[(\gamma - 1)/2]\bar{M}^2 J \tag{19}$$

where

$$J = \bar{p}\int \frac{s'}{R} S\,\mathrm{d}x \tag{20}$$

The mass, momentum, and energy of an entropy pulse are thus all proportional to the entropy integral J that has the dimensions of energy and will be called the strength of the pulse. Because a pure entropy pulse is isobaric, only the temperature variation will contribute to the value of J. If the entropy pulse happens to be overlapped by an acoustic pulse, there will be a nonzero pressure contribution in Eq. (16), as necessary for the correct calculation of the entropy.

Note that the energy of an entropy pulse is purely kinetic and has no contribution from the internal energy. The internal energy ($\sim$pressure) disturbance is zero while the signs of the density and kinetic energy disturbances are opposite to that of the temperature change. The peculiar end result is that a hot spot in a stationary gas has no energy at all and a hot slug moving at the speed of the gas represents a negative total energy disturbance.

Analysis of Trigger Process

The trigger process consists of adding some combination of mass, momentum, and energy to the CV in a region of length λ_t during a time interval τ_t (shaded region in bottom part of Fig. 1). We assume that no disturbances are present before triggering, which means that the integrals of Eqs. (5–7) at time t_i are all zero:

$$W_i' = P_i' = H_i' = 0 \tag{21}$$

After the trigger process is completed, three pulses are present. The values of integrals appearing in Eqs. (5–7) at time t_f are given as the sums of three discrete contributions, one from each pulse:

$$W_f' = W_-' + W_+' + W_E' \tag{22}$$

$$P_f' = P_-' + P_+' + P_E' \tag{23}$$

$$H_f' = H_-' + H_+' + H_E' \tag{24}$$

Using Eqs. (10–12), (17–19), and (21–24), Eqs. (5–7) can be written as

$$I_- + I_+ - (\gamma - 1)\, J = \bar{a}^2 \Delta W \tag{25}$$

$$(\bar{M} - 1) I_- + (\bar{M} + 1) I_+ - [(\gamma - 1)\bar{M}] J = \bar{a} \Delta P \tag{26}$$

$$\left[\left(1 + \frac{\gamma - 1}{2}\bar{M}^2\right) \Big/ (\gamma - 1) - \bar{M}\right] I_- + \left[\left(1 + \frac{\gamma - 1}{2}\bar{M}^2\right) \Big/ (\gamma - 1) + \bar{M}\right] I_+ - \left(\frac{\gamma - 1}{2}\bar{M}^2\right) J = \Delta H \tag{27}$$

Equations (25–27) constitute a nonhomogeneous set of three linear equations for the three unknown pulse strengths I_+, I_-, and J. Given ΔW, ΔP, and ΔH, the solution is straightforward. In the possession of the strengths, all integral properties of the pulses are readily calculated.

The lengths and durations of the pulses are also important properties. Knowing the spatial extent and duration of the trigger region, these can be estimated by simple kinematic considerations, as illustrated in Fig. 1. The leading edge of a right acoustic pulse is assumed to originate at $t = 0$, $x = +\lambda_t/2$, and the trailing edge at $t = \tau_t$, $x = -\lambda_t/2$. This assumption, together with the known wave speeds, defines both the duration and the length of the pulses ($\lambda_\pm$, λ_E, and τ_+ are shown in Fig. 1). Completely analogous considerations apply to the left-moving acoustic and entropy pulses. Because strength is proportional to the product of the length and the amplitude, knowledge of the length immediately yields an estimate of the amplitude.

Heat Addition

Perhaps the simplest method to generate a pulse is abrupt heat addition, which is used here as an example. This process adds no mass and no momentum; therefore,

$$\Delta H = Q, \qquad \Delta W = \Delta P = 0 \tag{28}$$

Using Eqs. (25–27), the following remarkably simple results are obtained:

$$I_- = [(\gamma - 1)/2]Q, \qquad I_+ = [(\gamma - 1)/2]Q, \qquad J = Q \tag{29}$$

As expected, heat addition produces all three pulse types. The strengths are independent of the undisturbed Mach number. The strengths of the left- and right-moving acoustic pulses are the same, but the lengths of the pulses are not. Assuming, for simplicity, that λ_t is zero, then the durations of all pulses are equal to τ_t, and simple calculation shows that

$$\lambda_-/\lambda_+ = (1 - \bar{M})/(1 + \bar{M}) \tag{30}$$

The left-moving acoustic pulse is thus shorter than the right-moving pulse, and because the strengths are the same, its amplitude is correspondingly higher. This is true for the slightly more complicated case of finite λ_t also.

The distribution of the total disturbance energy among the product pulses is a fundamental question to which the present theory offers a very clear answer. Having calculated the strengths, Eqs. (12) and (19) are used to find the fractions of energy as

$$H_\pm'/Q = \tfrac{1}{2} \pm [(\gamma - 1)/2]\bar{M} + [(\gamma - 1)/4]\bar{M}^2 \tag{31}$$

$$H_E'/Q = -[(\gamma - 1)/2]\bar{M}^2 \tag{32}$$

These results are quite surprising. The strengths of the two acoustic pulses are the same, yet the energies associated with them are different. The right-moving pulse carries more energy, despite the fact that its amplitude is lower than that of the left-moving pulse. The difference is derived from the kinetic energy contributions and becomes greater as the Mach number increases. The combined energy of the two acoustic pulses is more than the energy added in the trigger event, but the energy balance is still satisfied because the entropy pulse is associated with an energy deficiency. This energy allocation picture is highly counterintuitive and was unexpected at the outset of this work.

Comparisons for the Heat-Addition Case

Abrupt heat addition was used in a recent experiment[3,5] to generate the pulses needed to measure the impedance of an operating compressor with the impulse method. Heat was added to the inlet duct flow by passing a current pulse through a thin wire stretched along a diameter. The relationship between pulse properties and the energy added was a side issue for this project, but a limited amount of relevant data was nevertheless obtained.[7] Figure 2 shows the strength of the downstream-moving pulses against energy input. The predicted dependence on heat input and the independence of Mach number are clearly demonstrated by the data.

The present results agree very well with numerical simulations also. Two computational fluid dynamics (CFD) codes were used, both of which solve the unsteady continuity, momentum, and energy equations for a perfect gas over a quasi-one-dimensional flow domain. LAPIN[8] uses a finite difference discretization with a time-marching method that can transition between explicit and implicit and a conservative, shock-capturing method using characteristic information. QUAS1D, which was developed by the third author, uses a finite volume discretization with an explicit Lax–Wendroff time-marching algorithm and Roe upwind flux-difference splitting. The assumptions made in the analysis are closely satisfied by both codes.

Uniform step sizes were used in both distance and time. Grid-resolution studies were made for both codes to validate the final choices of the time and spatial step sizes. Duct lengths were chosen sufficiently long to ensure that reflections from the duct ends did not contaminate the results. Because the codes are fully nonlinear, deviations from the present results increased with disturbance amplitude. Computations were carried out for three amplitudes and

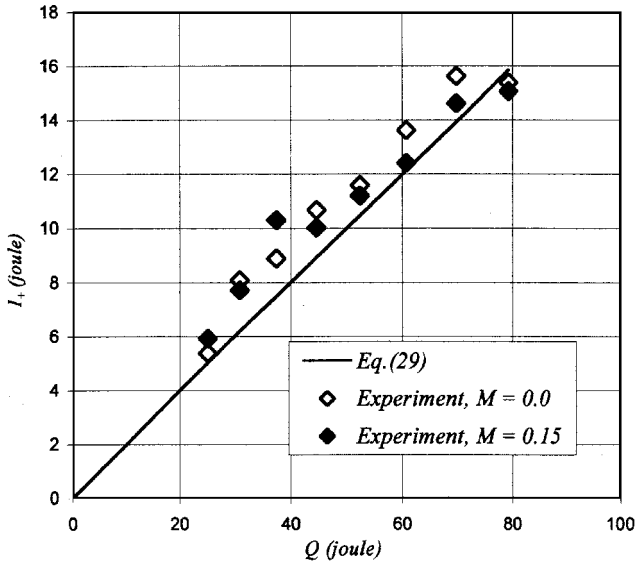

Fig. 2 Comparison of predicted strengths of right-moving acoustic pulses created by heat addition with experimental data: $S = 153.3\ \text{cm}^2$, $\gamma = 1.4$, and $\bar{a} = 345$ m/s.

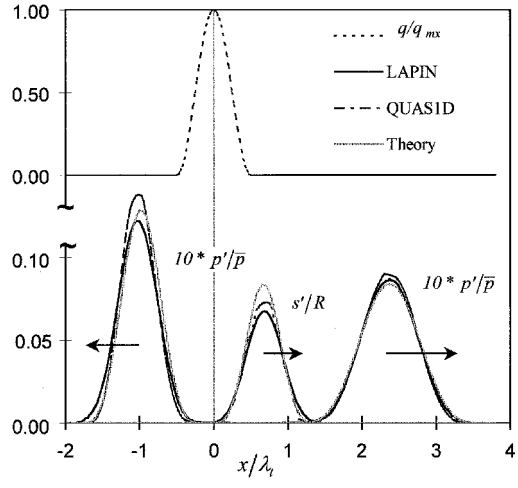

Fig. 3 Comparison of predicted pulses with CFD results for pulses created by heat addition, at time $t/\tau_t = 2.0$. Top curve illustrates the spatial distribution of heat flow rate per unit length at time $t/\tau_t = 0.5$. $Q/H_t = 0.01614$, and $\bar{M} = 0.4$.

three Mach numbers. The rate of heat addition per unit duct length was defined by the following expression:

$$q(x,t) = q_{\text{mx}} \cos^2[\pi(x/\lambda_t)] \sin^2[\pi(t/\tau_t)]$$
$$-0.5 \le x/\lambda_t \le 0.5, \qquad 0 \le t/\tau_t \le 1 \quad (33)$$

By integrating this expression over both space and time, the total heat added is obtained as

$$Q = \tfrac{1}{4} q_{\text{mx}} \lambda_t \tau_t \quad (34)$$

The heat addition is referenced to the static internal energy in the trigger volume:

$$H_t = c_v \bar{T}(\bar{\rho}\lambda_t S) = \bar{p}\lambda_t S/(\gamma - 1) \quad (35)$$

Figure 3 illustrates the three pulses created, as predicted by the two codes and by the current theory for $\bar{M} = 0.4$ and $Q/H_t = 0.01614$. For the analytical prediction the pulse shapes were described as the fourth power of a cosine curve from $-\pi/2$ to $+\pi/2$. By pure chance, this function is a very good fit to the numerically calculated shapes. The vertical scale was determined from the kinematic pulse length estimate, by matching the analytically predicted pulse strengths. The analytical pulse locations, amplitudes, and pulse lengths are all in excellent agreement with both codes, for all three pulses. Because the codes are fully nonlinear, the deviations increased with Q, as expected. For normalized heat inputs less than 4% and for Mach numbers 0.15, 0.3, and 0.45, the deviations between the analytically and numerically obtained strength values are within 0–1% for I_+ and I_- and within ±2% for J.

Abrupt Deformation of Duct Wall

It is possible to extend this method to describe the effects of an abrupt deformation of a short duct segment. The details are lengthy and omitted, but the concept is straightforward and will be outlined next.

A short, small area variation ("bump") within a steady flow creates no axial momentum disturbance, but it does give rise to local, stationary disturbances of mass and energy, which can be readily computed using the linearized forms of the isentropic, one-dimensional duct flow relations. In evaluating these quantities, the area variation is expressed as a sum of the constant duct area plus a disturbance ($S = \bar{S} + S'$). Omitting details, the mass and energy disturbances are

$$W'_B = \frac{\gamma}{(1-\bar{M}^2)\bar{a}^2} B \quad (36)$$

$$H'_B = \left[\left(\frac{\gamma}{\gamma - 1} \right) \cdot \left(1 - \frac{\gamma - 1}{2} \bar{M}^2 \right) \Big/ (1 - \bar{M}^2) - 1 \right] B \quad (37)$$

where

$$B = \bar{p} \int S' \, \mathrm{d}x \quad (38)$$

The quantity B is proportional to the volume associated with the deformation and is called here the strength of the bump. Pulses can be initiated by a change in the strength of the bump. Such a change does not alter the mass or momentum within the CV, and we have

$$\Delta W = 0, \qquad \Delta P = 0 \quad (39)$$

The motion of the boundary does add energy to the gas. The work done by the boundary displacement on the gas is given approximately as

$$\Delta H = -\int \mathrm{d}x \int p \, \mathrm{d}S \cong -\bar{p} \int S'_f \, \mathrm{d}x + \bar{p} \int S'_i \, \mathrm{d}x$$
$$= -(B_f - B_i) = -\Delta B \quad (40)$$

The remaining derivation is similar to that of the preceding section. The only difference is that the presence of the bump leads to a new term in the integrals over the CV, increasing the number of discrete contributions from three to four. Depending on the values of B_f and B_i, stationary disturbances can be present either before or after the trigger process or even at both times. All of these must be added to Eqs. (5–7) and (21–24). In all cases the bump strengths are known inputs that are eventually incorporated in the forcing terms of the final equations.

Of special interest is the experimentally realized[3] "collapsing bump" case ($B_i < 0$, $B_f = 0$). Omitting some fairly lengthy details, the analytical results for this case are

$$I_- = -[\gamma/2(1-\bar{M})]\Delta B, \qquad I_+ = -[\gamma/2(1+\bar{M})]\Delta B$$
$$J = 0 \quad (41)$$

No entropy pulse is generated, which is reasonable because the transverse motion of the boundary performs no work by shear. Detailed examination of the results shows that the right-moving acoustic pulse is longer, has lower strength, and carries significantly more energy than the left-moving one. The bulk of total energy in the two pulses is derived from the initial, stationary disturbance caused by the bump (which is negative), whereas the work done on the gas during the collapse (also negative) plays a lesser role.

Simulations of a bump collapse were performed using the same CFD codes and methods as those described for the heat-addition case. Importantly, both codes are capable of properly treating rapidly moving solid boundaries.

The area disturbance history in this problem was represented by the expression

$$S'(x,t) = S'_i \cos^2[\pi(x/\lambda_t)]\cos^2[(\pi/2)(t/\tau_t)]$$
$$-0.5 \le x/\lambda_t \le 0.5, \qquad 0 \le t/\tau_t \le 1 \quad (42)$$

The initial bump strength is obtained by integrating over x at $t = 0$:

$$B_i = B(0) = \tfrac{1}{2}\bar{p}S'_i\lambda_t \quad (43)$$

For $\bar{M} = 0.15$, 0.3, and 0.45 and for $\Delta B/H_t$ up to 4%, the strengths calculated using Eqs. (41) agreed with the numerical results within ±1% for both right- and left-moving pulses.

Summary

A one-dimensional, linearized theory is presented for the rapid estimation of the properties of pulses generated in constant-area duct flows by events that can be modeled as abrupt and local additions of mass, momentum, or energy. The theory describes pulses by means of volume integrals of pressure or entropy disturbances (termed "strength") and also by length estimates obtained from kinematic considerations. The method is based on first principles and is capable of describing a variety of triggering mechanisms, two of which have been worked out in detail.

An abrupt addition of heat is shown to create two acoustic compression pulses and one entropy pulse, whose strengths are proportional to the amount of heat added. The combined energy of the two acoustic pulses is greater than energy added as heat, compensated for by the fact that the energy disturbance associated with the entropy pulse is negative. An abrupt, local change of the duct cross-sectional area creates two acoustic pulses, while no entropy pulse is generated. A local, abrupt area reduction creates compression pulses, whereas an area increase yields expansion pulses. The strength of the pulses is proportional to the change of duct volume associated with the wall geometry change.

The analytical predictions are confirmed by experimental data and show excellent agreement with computations performed using two different time-dependent Euler CFD codes.

Acknowledgment

The authors express their sincere thanks to A. B. Opalski for providing the experimental data used in Fig. 2.

References

[1]To, C. W. S., and Doige, A. G., "The Application of a Transient Testing Method to the Determination of Acoustic Properties of Unknown Systems," *Journal of Sound and Vibration*, Vol. 71, No. 4, 1982, pp. 545–554.

[2]Freund, D., and Sajben, M., "Reflection of Large Amplitude Acoustic Pulses from an Axial Flow Compressor," *Journal of Propulsion and Power*, Vol. 16, No. 3, 2000, pp. 406–414.

[3]Opalski, A. B., and Sajben, M., "Inlet/Compressor System Response to Short-Duration Acoustic Disturbances," *Journal of Propulsion and Power*, Vol. 18, No. 4, 2002, pp. 922–932.

[4]Freund, D., and Sajben, M., "Compressor-Face Boundary Condition Experiment: Generation of Acoustic Pulses in Annular Ducts," AIAA Paper 96-2657, July 1996.

[5]Opalski, A. B., and Sajben, M., "High Speed Inlet/Compressor System Response to Short-Duration Acoustic and Entropy Disturbances," AIAA Paper 2002-0372, Jan. 2002.

[6]Atassi, H. M., "Unsteady Aerodynamics of Vortical Flows: Early and Recent Developments," *Aerodynamics and Aeroacoustics*, edited by K. Y. Fung, Advanced Series on Fluid Mechanics, World Scientific Publishing, River Edge, NJ, 1994, pp. 121–171.

[7]Opalski, A. B., "Experimental Investigation of Rapid Flow Transients in an Inlet/Compressor System, Induced by Short-Duration Acoustic and Entropy Disturbances," Ph.D. Dissertation, Dept. of Aerospace Engineering and Engineering Mechanics, Univ. of Cincinnati, Cincinnati, OH, May 2002.

[8]Paynter, G. C., Clark, L. T., and Cole, G. L., "Modeling the Response from a Cascade to an Upstream Acoustic Disturbance," *AIAA Journal*, Vol. 38, No. 8, 2000, pp. 1322–1330.

H. M. Atassi
Associate Editor

Vortex Shedding and Transition Frequencies Associated with Flow Around a Circular Cylinder

N. A. Ahmed* and D. J. Wagner†
University of New South Wales,
Sydney, New South Wales 2052, Australia

Nomenclature

D	=	diameter of circular cylinder
f_s, f_V	=	shear-layer frequency and vortex-shedding frequency
Re	=	Reynolds number
Sr	=	Strouhal number
U_∞, U_{sep}	=	velocity of freestream and velocity at separation
u_{rms}	=	rms velocity
v	=	kinematic viscosity
x, y	=	coordinates of a Cartesian system
δ_x	=	displacement thickness

Introduction

FLOW around a circular cylinder has been studied for a long time,[1] and yet our knowledge, at best, is empirical. Of particular interest is the relationship between the ways that the Strouhal number varies with the Reynolds number for a circular cylinder flow. Above a Reynolds number of 10^3, transition to turbulence occurs in a separating shear layer, which is closely tied to the generation of large-scale vortices. Bloor[2] measured the frequency of transition waves within $1.3 \times 10^3 < Re < 4.5 \times 10^4$ and attempted theoretically to derive the relationship between the ratio of the shear-layer transition frequency and the main vortex-shedding frequency. She argued that $f_s/f_V \propto Re^{0.5}$ within $4 \times 10^2 < Re < 2.5 \times 10^5$. Although some experimental results[2,3] fit this prediction well, others[4,5] do not. The purpose of this Note is, therefore, to revisit the preceding problem by observing the dominant frequencies in the transition Reynolds-number range.

Experiment

The 18 × 18 in. open-circuit wind tunnel[6] of the aerodynamic laboratory of the University of New South Wales was used. The experimental setup is shown in Fig. 1. The velocity of the wind tunnel was found to be uniform to within ±0.2% and a turbulence intensity of less than 0.2%. These figures were taken to indicate low acoustic errors associated with the tunnel. The speed of the wind tunnel could be varied between 0 and 25 m/s. Two hot-wire signals were sampled simultaneously, one to take the reading at a point and the other to act as a reference in phase. Thus one hot wire, buried into the model cylinder surface, was moved around to the different angular locations on the cylinder, keeping the same height above the surface, and another hot wire was traversed through the external field using a traversing mechanism.

Test Model

A circular cylinder of diameter 70 mm, with a recess on the surface of the cylinder, was manufactured. The cylinder itself consisted of three hollowed segments so that it could be assembled and disassembled easily enabling the hot wire to be put in and signal cable

Received 30 July 2001; revision received 11 November 2002; accepted for publication 18 November 2002.

*Senior Lecturer, School of Mechanical and Manufacturing Engineering.
†Graduate Student, School of Mechanical and Manufacturing Engineering.